A Robust Energy and Reserve Dispatch Model for Prosumer Microgrids Incorporating Demand Response Aggregators

Uyikumhe Damisa[1*], Nnamdi I. Nwulu[1], Yanxia Sun[1]

[1]Department of Electrical and Electronic Engineering Science, University of Johannesburg, Corner Kingsway and University Road, Auckland, Johannesburg, South Africa.

[*]uyikumhe@yahoo.com

Abstract: The uncertainty introduced by intermittent renewable energy generation and prosumer energy imports makes operational planning of renewable energy-assisted prosumer microgrids challenging. This is due to the difficulty in obtaining accurate forecasts of energy expected from these renewable energy sources and prosumers. Operators of such microgrids therefore require additional grid-balancing tools to maintain power supply and demand balance during grid operation. In this paper, the impact of demand response aggregators (DRA's) in a prosumer microgrid is investigated. This is achieved by developing and solving a deterministic mathematical formulation for the operational planning of the grid. Also, taking a cue from CAISO's proposed tariff revision which allows the state-of-charge of non-generator resources (like storage units) to be submitted as a bid parameter in the day-ahead market and permits scheduling coordinators of these resources to self-manage their energy limits and state-of-charge, the proposed formulation permits prosumers to submit battery energy content as a bid parameter and self-manage their battery energy limits. Furthermore, a robust counterpart of the model is developed. Both formulations are constrained mixed integer optimization problems which are solved using the CPLEX solver in Advanced Interactive Multidimensional Modelling System (AIMMS) environment. Results obtained from tests carried out on a hypothetical prosumer microgrid show that the operating cost of the microgrid reduces in the presence of DRA's. In addition, the storage facility owner may benefit from self-managing its energy limits, but this may cut the amount of grid-balancing resource available to the microgrid operator, thereby increasing the operating cost of the microgrid.

Keywords: Microgrid, robust optimization, operational dispatch, optimization, energy management, prosumers.

Nomenclature

Sets

t, T	Interval index, number of intervals
g, G	Diesel generator (DG) index, number of DGs
p, P	Prosumer index, number of prosumers
w, W	Wind turbine index, number of wind turbines
s, S	Solar system index, number of solar systems
d, D	Demand response aggregator (DRA) index, number of DRAs

Parameters

$E_{wt,w}^{FC,t}$	Forecasted energy from wind turbine w during interval t [kWh]
$E_{ss,s}^{FC,t}$	Forecasted energy from solar system s during interval t [kWh]

$E^{t}_{PRGen,p}$ Energy locally generated by prosumer p during interval t [kWh]

$E^{FC,t}_{Demand}$ Forecasted total demand during interval t (excluding prosumer demand) [kWh]

$E^{t}_{PRDem,p}$ Energy demand by prosumer p during interval t [kWh]

$SC_{DG,g}$ Fixed start-up cost of DG g [$]

$E^{min}_{DG,g}$ Minimum energy output of DG g [kWh]

$E^{max}_{DG,g}$ Maximum energy output of DG g [kWh]

r Ramp Up/Down coefficient

$CR^{t}_{DG,g}$ Cost of reserve from DG g in interval t [$]

a_g, b_g& c_g Fuel cost function coefficients of generator g [$/kW^{2}h]/[$/kWh]/ [$/h]

$E^{max}_{BatTxf,p}$ Maximum energy transferable from/to battery in prosumer p per interval [kWh]

$E^{min,t}_{Batt,p}$ Minimum content of battery in prosumer p in interval t [kWh]

$E^{max,t}_{Batt,p}$ Maximum content of battery in prosumer p in interval t [kWh]

η_p Charging/discharging efficiency of battery at prosumer p

$PR_{PBatRes,p}$ Cost per unit of reserve in battery at prosumer p [kWh]

E^{t}_{RUR} Required up reserve during interval t [kWh]

E^{t}_{RDR} Required down reserve during interval t [kWh]

E^{max}_{grid} Maximum energy from grid per interval [kWh]

PR_{grid} Cost per unit of reserve from grid [$]

C^{t}_{b} Cost of buying a unit of energy from the grid in interval t [$/kWh]

$E^{t}_{PRMaxCurt,p}$ Maximum Energy curtailment specified by prosumer p during interval t [kWh]

$C_{PRCurt,p}$ Cost per unit of energy curtailed by prosumer p [$/kWh]

$E^{t}_{DRAMaxCurt,d}$ Maximum Energy curtailment specified by DRA d during interval t [kWh]

$C_{DRACurt,d}$ Cost per unit of energy curtailed by DRA d [$/kWh]

$\Delta E^{-,t}_{wt,w}$ & $\Delta E^{+,t}_{wt,w}$ Maximum downward & upward variation from forecasted wind turbine w output energy in interval t [kWh]

$\Delta E^{-,t}_{ss,s}$ & $\Delta E^{+,t}_{ss,s}$ Maximum downward & upward variation from forecasted solar system s energy output in interval t [kWh]

$\Delta E^{+,t}_{Demand}$ & $\Delta E^{-,t}_{Demand}$ Maximum upward & downward variation from forecasted demand in interval t [kWh]

$\Delta E^{-,t}_{PRGen,p}$ & $\Delta E^{+,t}_{PRGen,p}$Maximum downward & upward variation from forecasted local generator output at prosumer p in interval t [kWh]

$\Delta E^{+,t}_{PRDem,p}$ & $\Delta E^{-,t}_{PRDem,p}$Maximum upward & downward variation from forecasted demand at prosumer p in interval t [kWh]

$E^{0}_{Batt,p}$ is initial energy content of battery [kWh]

Variables

E^{t}_{Bought} Energy bought from the grid during interval t [kWh]

$R^{t}_{DG,g}$ Scheduled reserve from DG during interval t [kWh]

$DR^{t}_{DG,g}$Scheduled down reserve from DG during interval t [kWh]

$E^{t}_{DG,g}$ Scheduled energy from DG g during interval t [kWh]

$S^{t}_{DG,g}$ On/Off status of DG g in interval t [binary]

$SUC^{t}_{DG,g}$Start-up cost of DG g in interval t [$]

$C^{t}_{DG,g}$ Cost function of DG g [$]

$E^{Sch,t}_{DRACurt,d}$ Scheduled energy curtailment for DRA d during interval t [kWh]

$CSch^{t}_{DRACurt,d}$ Cost of scheduled energy curtailment for DRA d in interval t [$/kWh]

$E^{t}_{PRCurt,p}$ Scheduled energy curtailment for prosumer p during interval t [kWh]

$CSch^{t}_{PRCurt,p}$ Cost of scheduled energy curtailment for prosumer p in interval t [$/kWh]

$E^{t}_{ToFroPBat,p}$ Energy transferred to/fro battery in prosumer p during interval t [kWh]

$E^{t}_{InBatt,p}$ Energy content of battery in prosumer p during interval t [kWh]

$R^{t}_{PBatRes,p}$ Scheduled reserve in battery at prosumer p during interval t [kWh]

$E^{t}_{ToFroPros,p}$Energy transferred to/from prosumer p during interval t [kWh]

$DR^{t}_{PRCurt,p}$Scheduled down reserve from curtailed load of prosumer p in interval t [kWh]

1. INTRODUCTION

A rapid rise in renewable energy penetration has been recorded in recent years due to the adverse environmental impact of burning fossil fuels, depletion of these fuels and government support for renewable energy integration. Owing to their unpredictable nature, energy generation from renewable sources like the wind and sun introduce additional uncertainty to power systems, thereby complicating power system planning. Intelligent electricity grids like the microgrid (MG) which is capable of interconnecting various unpredictable sources of electrical power have attracted public attention in recent times.[1] A microgrid operator (MGO) responsible for operating such grids is

faced with the challenge of balancing power supply and demand during grid operations. This difficulty intensifies when the microgrid contains prosumers within its network. Ancillary services, like the provision of reserves, serve to ensure power balance in the grid, but with the increased uncertainty of the modern-day grid, more reserve capacity is needed to ensure reliable operation of the grid.[2,3] An additional 3 – 10 % of regulative service is required for each megawatt of renewable energy (solar and/or wind) connected to the grid [4]. The use of demand-side resources, like flexible loads and storage units, to provide ancillary services has been studied extensively.

In Ref. 5, an analysis of various methods by which short-term stored energy resources can participate in the Midcontinent Independent System Operator (MISO) energy and ancillary services market was presented. The authors of Ref. 6 proposed a novel scheduling approach for batteries participating in a joint day-ahead, reserve and regulation market. Studies regarding the provision of grid ancillary services using electric vehicles have been reported in literature.[7,8,9,10] The use of data centres to provide grid ancillary services has also been reported in literature.[11,12] By virtue of their inherent ability to react promptly to grid frequency fluctuations, batteries can offer grid ancillary services.[13,14] In Ref. 15, frequency containment reserve was provided by battery storage systems. In Ref. 16, a collection of solar battery systems was used to provide primary control reserve whilst the batteries were simultaneously fulfilling their primary purpose. The implementation of direct control of flexible loads for the provision of a portion of the needed ancillary services to an isolated grid in Australia was reported in Ref. 17. A report on demand response providing contingency reserves is contained in Ref. 2.

The optimal co-scheduling of supply and demand-side resources for energy and reserve co-management has also attracted the attention of some researchers. A joint energy and reserve market model, where generators and consumers can offer or bid for energy and various reserve products, was proposed in Ref. 18. The authors concluded that reserve offers from demand-side resources add extra scheduling flexibility which can lead to substantial social welfare benefits. A microgrid interconnecting both conventional and renewable energy sources with industrial and commercial loads was investigated in Ref. 19. In the paper, customers are able to partake in energy and reserve provision using a variety of demand response programs. Day-ahead and near-real time schedules were developed in two stages, and tests were carried out on the microgrid test system. Microgrid operational cost was seen to decrease with the participation of consumers in the energy and reserve scheduling. In Ref. 1, a combination of diesel generators and load was used to provide the reserve capacity to compensate for the uncertainties in renewable generation which were modelled by probability distribution functions. The authors of the paper proposed a stochastic energy and reserve planning scheme, and results obtained from their case study corroborate results gotten in Ref. 19. Diesel generator usage was also found to be lower with the involvement of demand side resources. Customer participation in energy and reserve scheduling was investigated on a smart distribution network, in Ref. 20. Demand reduction offers from medium and small scale electricity consumers were aggregated by demand response aggregators, thereby enabling these relatively small consumers to indirectly participate in the reserve and energy scheduling process. Their results also showed a reduction in grid operating cost with the participation of demand side resources in energy and reserve scheduling. The authors of Ref. 21 proposed a stochastic energy and reserve management method for a renewable energy assisted microgird. In their scheme, resources from the main grid, dispatchable generators and demand response were used to compensate for the uncertainties in wind, solar and load. The aggregation of prosumer resources for the provision of ancillary services was proposed in Ref. 22. A renewable energy – assisted prosumer microgrid was taken as case study, and a day-ahead energy and reserve optimal schedule for dispatchable generation, flexible demand and prosumer batteries were generated. The microgrid operator's cost was seen to reduce with the involvement of prosumer behind-the-meter resources in the energy and reserve planning. In Ref. 22 however, the demand-side resources of large consumers alone were engaged in the operational planning of the microgrid; small and medium scale customers were neglected thereby depriving these customers of the benefits of participation, and robbing the MGO of additional grid-balancing resources. Moreover, the participation of these large customers gave the MGO only a limited level of flexibility as he could only switch on/off a fixed amount of load per time slot.

A crucial aspect of the development of an optimal energy dispatch model for power grids with intermittent resources is the approach to uncertainty modelling. Various methods have been proposed and explored in the literature. The scenario-based optimization method is one that has been used widely to model uncertainties. In Ref. 23, a joint energy and reserve optimal dispatch model which also determines the optimal topology of a microgrid is developed. Appropriate probability distribution functions (PDFs) are used to represent the stochastic nature of wind speed and load. Segmented PDFs are then used to generate scenarios which are utilized in the scheduling process. The resulting formulation is a mixed integer non-linear problem which is solved using a genetic algorithm. A multi-objective mixed integer linear model which minimizes microgrid operating cost and air pollution is presented in Ref. 24. Discretized PDFs for wind speed, solar irradiation and load are used to generate scenarios and the most probable ones are selected for use. To handle uncertainties in wind speed, solar power, load and electricity prices, the authors of Ref. 25 proposed a two-part scenario-based stochastic programming method. The Monte Carlo simulation with Latin Hypercube sampling method is used to generate various scenarios after forecasts have been obtained using a traditional forecasting procedure. To reduce computational time, a scenario reduction approach is implemented in the general algebraic modelling systems (GAMS). A two-stage stochastic programming model aimed at minimizing the investment and operation cost of a microgrid is developed in Ref. 26. Uncertainties in solar, wind and demand are modelled using the scenario tree approach. Simulations are carried out on the INER microgrids in Taiwanese market. Although the Monte Carlo simulation is considered a very accurate approach to uncertainty modelling, a large number of scenarios generated by the method increases the computational time.[23] Also, in real life applications, exact probability distribution functions may be difficult to obtain.[27]

The chance constrained programming technique is another approach to dealing with uncertainties in optimization problems. Ref. 28 proposed two energy management systems: one for frequency regulation and the other for peak shaving and system protection. With probabilistic constraints, a chance constrained optimization model is developed which handles uncertainties in renewable energy sources and demand in a grid-connected microgrid. The difficulty in solving chance constrained is a drawback of the approach.[29]; they are hardly tractable.[30]

Robust optimization approach has also been proposed and investigated in literature. A scenario-based robust energy optimization model which immunizes against the worst case realization of renewable power production and load is presented in Ref. 31. Interval prediction is used to generate an uncertainty set to handle uncertainty of load and renewables. In Ref. 32, a robust two-stage energy management model with the objective of minimizing long-term average grid operating cost is developed. Renewable generation and load uncertainties are represented by bounded uncertainty sets, and their worst case realizations are handled by the robust optimization technique. To minimize the operating cost of a microgrid under worst case realization of renewable generator output and grid connection condition, the authors of Ref. 33 proposed a two-stage robust energy management approach. In Ref. 34, with the aim of determining a robust optimal generation schedule and ensuring a feasible solution for all possible realizations of uncertainty, a robust optimization model is proposed for energy dispatch. Similarly, in Ref. 27, a robust model for the co-optimization of energy and ancillary services in real-time markets is proposed. Using the method of participation factors, optimal base points of generators are determined whilst ensuring that a feasible solution exists for any realization of uncertainty within a specified uncertainty set. Optimal solutions generated from the robust optimization approach are still fair even if the realization of uncertainty falls outside initially specified intervals.[35]. Robust optimization methodologies applied to uncertain linear problems can be computationally tractable, if certain conditions are met.

This paper proposes an operational planning formulation in which the resources of small and medium scale electricity consumers are able to partake in the operational planning via demand response aggregators (DRA's), as in Ref. 20. The inclusion of DRA's is important because they offer benefits to customers as well as the MGO; small and medium-scale customers get paid for reducing demand, and the MGO gets more scheduling flexibility. Also, in contrast with the mode of participation of large electricity customers proposed in Ref. 22, large customers (assumed to be prosumers who own storage facilities) submit load reduction offers, as in Ref. 1. This enhances flexibility for

the large customers as well as the MGO. While in Ref. 22, only the up-reserve capacity was provided for, the proposed formulation in this paper also caters for a down-reserve capacity for situations when renewable generation overshoots forecasted values and/or forecasted demand exceeds actual demand. The required up-reserve capacity is provided by DGs and prosumer batteries, and down-reserve is made available using DGs and prosumer load curtailments. The key point of deviation of this paper from other works reported in literature is the leeway given to prosumers to submit battery energy content (which is related to the state of charge of charge of the battery) as a bid parameter and self-manage their battery energy limits. This is in line with CAISO's proposed tariff revisions which allows the state-of-charge of non-generator resources like storage units to be submitted as a bid parameter in the day-ahead market, and permits scheduling coordinators of these resources to self-manage their energy limits and state-of-charge.[36] Furthermore, a robust model is developed to deal with uncertainties in the microgrid's wind power, solar power and demand. The proposed formulation is meant to be used by a MGO who obtains forecasts for renewable energy generation, electricity price and demand, generation offers from DGs, and load reduction offers from prosumers and DRA's. With these data, the MGO generates an optimal operational day-ahead energy and reserve schedule for the microgrid. The main contributions of this paper can be summarized as follows:

- A revision proposed by CAISO regarding the participation of non-generator resources in the electricity market is investigated on a prosumer microgrid.
- A robust model for energy and reserve dispatch for a prosumer microgrid incorporating DRA's is developed.

The rest of the paper is organized as follow: the microgrid architecture is described in Section 2, and the mathematical models are developed in Section 3. In Section 4, a description of the simulation setup is given, and results obtained are reported in Section 5. The results are discussed in Section 6, and the paper is concluded in Section 7.

2. SYSTEM ARCHITECTURE

Fig. 1 is a schematic of a prosumer microgrid within the network of a distribution system. It indicates the interactions between the MGO and other grid components. The communication link between the DSO and MGO is used by the DSO to communicate main grid electricity prices to the MGO, while the same channel is used by the MGO to communicate day-ahead scheduled grid energy purchase after optimal energy schedules have been generated. DGs send generation offers to the MGO while DRA's and prosumers submit bid parameters which include maximum possible energy curtailment per interval and price per unit of energy curtailed to the MGO. These data together with other data like renewable energy output forecasts are used to perform optimal scheduling of these resources. Schedules for DGs and Prosumers are sent to their respective local controllers, while that for DRA's are sent to the respective DRA's who then send the information or control signals to the local controllers of flexible loads. The MGO pays the DRA for this service, while the customers with flexible loads receive remuneration from their DRA. Various wireless and wired technologies have been proposed for communication among microgrid components..[37] Fig. 2 shows the proposed communication architecture for the microgrid network. General packet radio service (GPRS) is proposed for communication between the MGO and both the DRA's and DSO, while prosumers make use of power line communication for communication with the MGO.

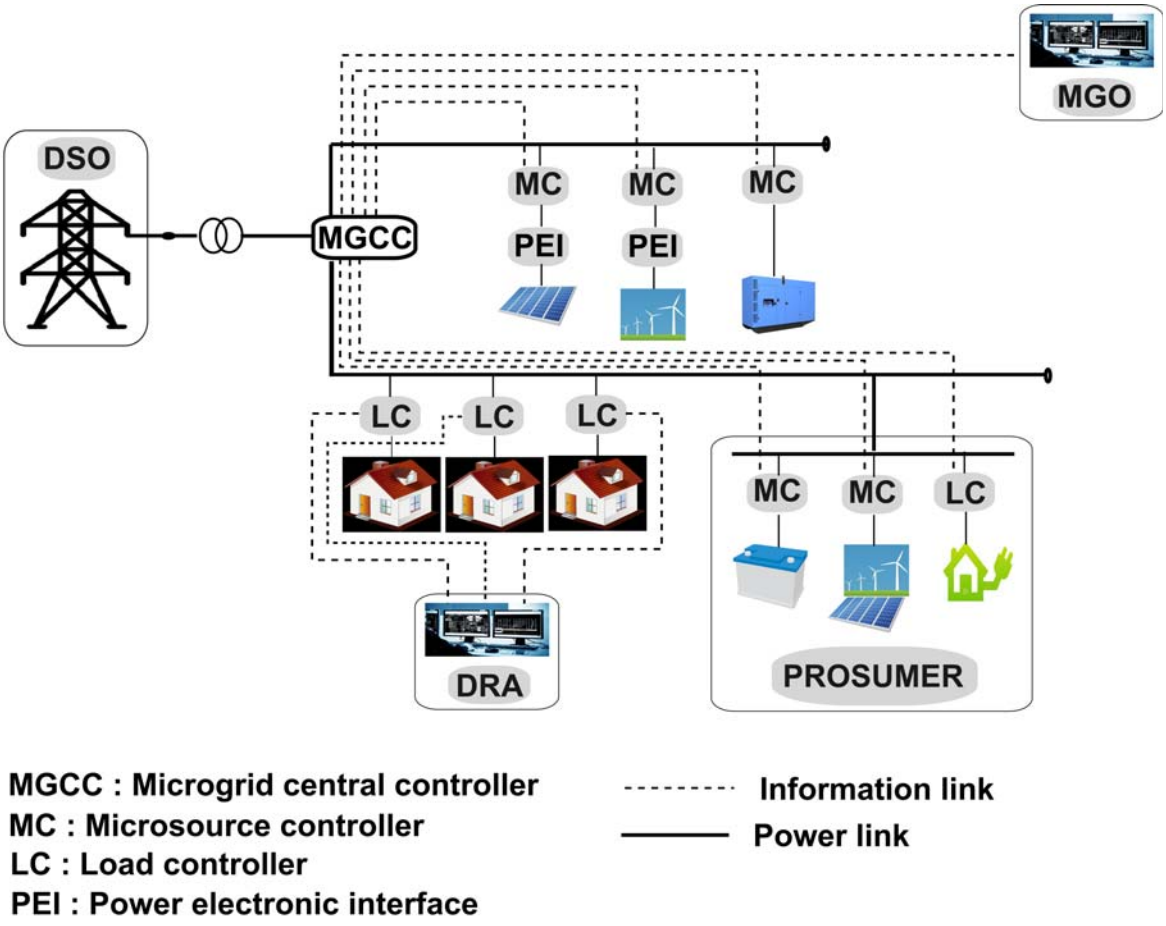

Fig. 1 System architecture

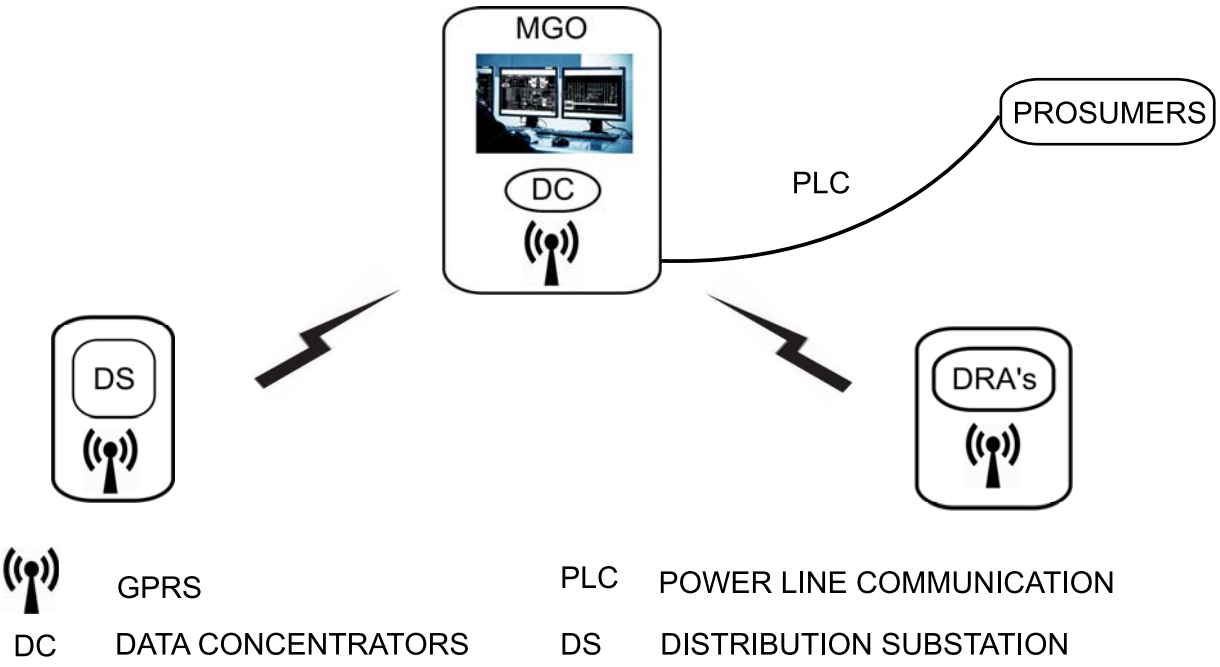

Fig. 2 Communication architecture

3 Mathematical Modelling

3.1 Deterministic Optimization Model

3.1.1 Objective Function

The expression in (1) depicts the MGO's cost metric, and doubles as the objective function of the proposed optimization model. It comprises the cost of scheduled energy and reserve from various grid and prosumer resources.

$$\sum_{t=1}^{T}(C_b^t * E_{Bought}^t) + \sum_{t=1}^{T}\sum_{g=1}^{G} C_{DG,g}^t) + \sum_{t=1}^{T}\sum_{g=1}^{G} CR_{DG,g}^t + \sum_{t=1}^{T}\sum_{g=1}^{G} SUC_{DG,g}^t + \sum_{t=1}^{T}\sum_{d=1}^{D} CSch_{DRACurt,d}^t + \sum_{t=1}^{T}\sum_{p=1}^{P} CSch_{PRCurt,p}^t + \sum_{t=1}^{T}\sum_{p=1}^{P}(R_{PBatRes,p}^t * PR_{PBatRes,p}) \quad (1)$$

Where:

$$C_{DG,g}^t = S_{DG,g}^t * a_g + b_g * E_{DG,g}^t \quad \forall\, t \in [1, T]\ \forall\, g \in [1, G] \quad (2)$$

$$CR_{DG,g}^t = 0.62 * (S_{DG,g}^t * a_g + b_g * R_{DG,g}^t) \quad \forall\, t \in [1, T]\ \forall\, g \in [1, G] \quad (3)$$

$$CR_{Batt,s}^t = 0.01 * C_b^t * R_{Batt,s}^t \quad \forall\, t \in [1, T]\ \forall\, g \in [1, G] \quad (4)$$

3.1.2 Constraints

Each time a DG comes on, a start-up cost is incurred which is enforced using constraints (5) and (6).[1]

$$SUC_{DG,g}^t \geq SC_{DG,g} * \left(S_{DG,g}^t - S_{DG,g}^{t-1}\right) \quad \forall\, t \in [1, T]\ \forall\, g \in [1, G] \quad (5)$$

$$SUC^{t}_{DG,g} \geq 0 \quad \forall\, t \in [1, T] \;\; \forall\, g \in [1, G] \tag{6}$$

Constraint (7) ensures that DGs are not scheduled to operate outside their operating range.

$$S^{t}_{DG,g} * E^{min}_{DG,g} \leq E^{t}_{DG,g} + R^{t}_{DG,g} \leq E^{max}_{DG,g} * S^{t}_{DG,g} \;\; \forall\, t \in [1, T] \; \forall\, g \in [1, G] \tag{7}$$

DG ramp rate constraints are enforced using constraints (8) and (9); the first being the upward ramp rate constraint and the second being the downward ramp rate constraint.

$$E^{t}_{DG,g} + R^{t}_{DG,g} - E^{t-1}_{DG,g} - R^{t-1}_{DG,g} \leq r * E^{max}_{DG,g} \;\; \forall\, t \in (1, T] \;\; \forall\, g \in [1, G] \tag{8}$$

$$E^{t-1}_{DG,g} + R^{t-1}_{DG,g} - E^{t}_{DG,g} - R^{t}_{DG,g} \leq r * E^{max}_{DG,g} \;\; \forall\, t \in (1, T] \;\; \forall\, g \in [1, G] \tag{9}$$

The scheduled down-reserve per interval to be provided by a DG should not exceed its downward ramp rate, hence the need for constraint (10). Also, the current operating point of a DG limits the amount of down-reserve that it can deliver, as described by constraint (11)

$$DR^{t}_{DG,g} \leq r * E^{max}_{DG,g} \;\; \forall\, t \in [1, T] \; \forall\, g \in [1, G] \tag{10}$$

$$DR^{t}_{DG,g} \leq \left(E^{t}_{DG,g} - S^{t}_{DG,g} * E^{min}_{DG,g}\right) \forall\, t \in [1, T] \; \forall\, g \in [1, G] \tag{11}$$

DRAs submit bids to the MGO who performs the optimal day-ahead schedule for the microgrid. Bid parameters sent include maximum load curtailable per interval and cost per KWh of load curtailed. Constraint (12) keeps the scheduled load curtailment per interval within the specified permissible level, and the total cost of scheduled energy curtailment is obtained from equation (13)

$$E^{t}_{DRACurt,d} \leq E^{t}_{DRAMaxCurt,d} \quad \forall\, t \in [1, T] \;\; \forall\, d \in [1, D] \tag{12}$$

$$CSch^{t}_{DRACurt,d} = E^{t}_{DRACurt,d} * C_{DRACurt,d} \;\; \forall\, t \in [1, T] \;\; \forall\, d \in [1, D] \tag{13}$$

Prosumers set the maximum load curtailable per interval and the cost per KWh of curtailed load. This data is transmitted to the MGO via the SCADA system. Constraint (14) keeps the level of scheduled load curtailment per interval within the specified boundary, and the total cost of scheduled energy curtailment is obtained from equation (15)

$$E^{t}_{PRCurt,p} \leq E^{t}_{PRMaxCurt,p} \; \forall\, t \in [1, T] \;\; \forall\, p \in [1, P] \tag{14}$$

$$CSch^{t}_{PRCurt,p} = E^{t}_{PRCurt,p} * C_{PRCurt,d} \; \forall\, t \in [1, T] \;\; \forall\, p \in [1, P] \tag{15}$$

Since power can be readily restored to loads from which power was initially withdrawn, energy curtailed can be viewed as a down-reserve capacity. Hence, in the proposed model, one of the components that make up the required down reserve capacity per time interval is the total prosumer energy curtailed. Constraint (16) ensures that this component does not exceed the scheduled amount of energy curtailment.

$$DR^{t}_{PRCurt,p} \leq E^{t}_{PRCurt,p} \; \forall\, t \in [1, T] \;\; \forall\, p \in [1, P] \tag{16}$$

Each prosumer is assumed to have a battery storage facility co-located with the onsite renewable energy generator, and equation (17) describes the battery dynamics across intervals. At time t = 1, $E^{t-1}_{Batt,p} = E^{0}_{Batt,p}$ which represents the initial energy content of the battery.

$$E^{t}_{Batt,p} = E^{t-1}_{Batt,p} + \eta_{p}\left(E^{t}_{ToFroPBat,p}\right) - \eta_{p}\left(R^{t}_{Batt,p}\right) \;\; \forall\, p \in [1, P] \; \forall\, t \in [1, T] \tag{17}$$

Constraint (18) ensures that the battery energy content per interval remains within its capacity range.

$$E^{min,t}_{Batt,p} \leq \ E^{t}_{Batt,p} \leq \ E^{max,t}_{Batt,p} \ \forall\ p \in [1, P] \ \forall\ t \in [1, T] \tag{18}$$

Constraints (19) through (21) ensure that the total scheduled energy and reserve per interval do not exceed the maximum discharge energy amount per interval

$$-E^{max}_{Txf,p} \leq \ E^{t}_{ToFroPBat,p} \quad \forall\ p \in [1, P] \ \forall\ t \in [1, T] \tag{19}$$

$$-E^{t}_{ToFroPBat,p} + R^{t}_{Batt,p} \ \leq \ E^{max}_{Txf,p} \ \forall\ p \in [1, P] \ \forall\ t \in [1, T] \tag{20}$$

$$E^{t}_{ToFroPBat,p} + R^{t}_{Batt,p} \ \leq \ E^{max}_{Txf,p} \ \forall\ p \in [1, P] \ \forall\ t \in [1, T] \tag{21}$$

Only a portion of a battery's content can be utilized; the balance is lost to battery inefficiency. This effect is enforced by constraint (22).

$$\eta_p E^{t-1}_{Batt,p} \geq -E^{t}_{ToFroPBat,p} + R^{t}_{Batt,p} \ \forall\ p \in [1, P] \ \forall\ t \in [1, T] \tag{22}$$

Equation (23) is the energy balance constraint at prosumer's incoming/outgoing node.

$$E^{t}_{PRGen,p} + E^{t}_{PRCurt,p} + E^{t}_{ToFroPros,p} = E^{t}_{PRDem,p} + E^{t}_{ToFroPBat,p} \ \forall\ t \in [1, T] \ \forall\ p \in [1, P] \tag{23}$$

The total energy imported into the MG per interval is limited by the size of the incoming transformer, hence the need for constraint (24)

$$E^{t}_{Bought} \leq E^{max}_{grid} \quad \forall\ t \in [1, T] \tag{24}$$

To ensure a balanced system, equation (25) is enforced.

$$\sum_w^W E^{FC,t}_{wt,w} + \sum_s^S E^{FC,t}_{ss,s} + E^{t}_{Bought} + \sum_g^G E^{t}_{DG,g} + \sum_d^D E^{Sch,t}_{DRACurt,d} - E^{FC,t}_{Demand} - \sum_p^P E^{t}_{ToFroPros,p} = 0 \ \forall\ t \in [1, T] \tag{25}$$

The required up-reserve capacity is the sum of maximum downward variation in wind and solar power forecast and upward variation of demand, as shown in equation (26). This capacity is jointly catered for by the main grid, DGs and prosumers' batteries, as indicated in constraint (27)

$$E^{t}_{RUR} = \sum_w^W \Delta E^{-,t}_{wt,w} + \sum_s^S \Delta E^{-,t}_{ss,s} + \Delta E^{+,t}_{Demand} + \sum_p^P \Delta E^{-,t}_{PRGen,p} + \sum_p^P \Delta E^{+,t}_{PRDem,p} \ \forall\ t \in [1, T] \tag{26}$$

$$\sum_g^G R^{t}_{DG,g} + \sum_p^P R^{t}_{PBatRes,p} \geq E^{t}_{RUR} \ \forall\ t \in [1, T] \tag{27}$$

The required down-reserve capacity is the sum of maximum upward variation in wind and solar power forecast and downward variation of demand, as shown in equation (28). This capacity is jointly catered for by the DGs and curtailed prosumer loads, as indicated in constraint (29)

$$E^{t}_{RDR} = \sum_w^W \Delta E^{+,t}_{wt,w} + \sum_s^S \Delta E^{+,t}_{ss,s} + \Delta E^{-,t}_{Demand} + \sum_p^P \Delta E^{+,t}_{PRGen,p} + \sum_p^P \Delta E^{-,t}_{PRDem,p} \ \forall\ t \in [1, T] \tag{28}$$

$$\sum_g^G DR^{t}_{DG,g} + \sum_p^P DR^{t}_{PRCurt,p} \geq E^{t}_{RDR} \ \forall\ t \in [1, T] \tag{29}$$

Where:

$$\text{Percentage forecast error} = \left(\frac{\text{Actual} - \text{Forecast}}{\text{Actual}}\right) * 100 \tag{30}$$

$$\text{Actual} = \frac{100 * \text{Forecast}}{100 - \text{Percentage forecast error}} \tag{31}$$

$$\Delta = \text{Actual} - \text{Forecast} \tag{32}$$

3.1.3 Wind and Solar Power Output

Power output from the solar panels and wind turbines are calculated from the average of solar irradiance and wind speed forecasts respectively, as follows: (also used in Ref. 1):

$$P_{pv}(\emptyset) = \eta^{pv} * S^{pv} * \emptyset \tag{33}$$

$P_{pv}(\emptyset)$, η^{pv}, S^{pv} and $\emptyset$ represent solar panel power output, solar panel efficiency, solar panel surface area and average solar irradiance, respectively.

$$P_w(v) = \begin{cases} 0, & 0 \le v_a \le v_{ci} \\ P_{rated} * \frac{(v_a - v_{ci})}{(v_r - v_{ci})}, & v_{ci} \le v_a \le v_r \\ P_{rated}, & v_r \le v_a \le v_{co} \\ 0, & v_{co} \le v_a \end{cases} [1] \tag{34}$$

$P_w(v)$ and P_{rated}, represent wind turbine power output and power rating respectively. v_{ci}, v_{co} & v_a represent wind turbine cut-in and cut-out speeds and average wind speed respectively.

3.2 Robust Optimization Model

Taking a cue from the use of participation factors and base point generation schedules in Ref. 27, each DRA is assigned a participation factor γ_d and base point curtailment schedule $E^{sch,t}_{DRACurt,d}$. The participation factor determines how much increase/decrease of each DRA's load curtailment is required to achieve power balance, after realization of uncertain parameters. Forecast errors for wind, solar and demand are $eE^{t}_{wt,w}$, $eE^{t}_{ss,s}$ and eE^{t}_{Demand} and are within ranges [$eE^{min}_{wt,w}$, $eE^{max}_{wt,w}$], [$eE^{min}_{ss,s}$, $eE^{max}_{ss,s}$] and [eE^{min}_{Demand}, eE^{max}_{Demand}] respectively. Forecast error determination follows the convention used in (32).

Let α be the sum of forecast errors of wind, solar and demand forecasts. Hence,

$$\alpha = \sum_w^W eE^{t}_{wt,w} + \sum_s^S eE^{t}_{ss,s} - eE^{t}_{Demand} \tag{35}$$

$$\alpha^{max} = \sum_w^W eE^{max}_{wt,w} + \sum_s^S eE^{max}_{ss,s} - eE^{min}_{Demand} \tag{36}$$

$$\alpha^{min} = \sum_w^W eE^{min}_{wt,w} + \sum_s^S eE^{min}_{ss,s} - eE^{max}_{Demand} \tag{37}$$

The actual load curtailment after realization of wind, solar and load, $E^{Act,t}_{DRACurt,d}$, is adjusted from the scheduled value using the participation factor as shown in (38)

$$E^{Act,t}_{DRACurt,d} = E^{sch,t}_{DRACurt,d} - \gamma_d \alpha \quad \forall\, d \in [1, D] \tag{38}$$

After realization of α , the energy balance equation, (25), becomes (39).

$$\sum_w^W (E^{FC,t}_{wt,w} + eE^{t}_{wt,w}) + \sum_s^S (E^{FC,t}_{ss,s} + eE^{t}_{ss,s}) + E^{t}_{Bought} + \sum_g^G E^{t}_{DG,g} + \sum_d^D (E^{Sch,t}_{DRACurt,d} - \gamma_d \alpha) - E^{FC,t}_{Demand} - eE^{t}_{Demand} - \sum_p^P E^{t}_{ToFroPros,p} = 0 \quad \forall\, t \in [1, T] \tag{39}$$

$$\sum_w^W E^{FC,t}_{wt,w} + \sum_s^S E^{FC,t}_{ss,s} + E^{t}_{Bought} + \sum_g^G E^{t}_{DG,g} + \sum_d^D E^{Sch,t}_{DRACurt,d} - E^{FC,t}_{Demand} - \sum_p^P E^{t}_{ToFroPros,p} + \sum_w^W eE^{t}_{wt,w} + \sum_s^S eE^{t}_{ss,s} - \sum_d^D \gamma_d \alpha - eE^{t}_{Demand} = 0 \quad \forall\, t \in [1, T] \tag{40}$$

Inserting (25) in (40), (41) is obtained.

$$\sum_{w}^{W} eE_{wt,w}^{t} + \sum_{s}^{S} eE_{ss,s}^{t} - eE_{Demand}^{t} - \sum_{d}^{D} \gamma_d \alpha = 0 \quad \forall\, t \in [1, T] \tag{41}$$

$$\alpha - \sum_{d}^{D} \gamma_d \alpha = 0 \tag{42}$$

$$\left(1 - \sum_{d}^{D} \gamma_d\right)\alpha = 0 \tag{43}$$

$$\sum_{d}^{D} \gamma_d = 1 \tag{44}$$

Hence, energy balance is ensured for any realization of α if (44) is satisfied.

To ensure a feasible solution for any realization of α, (45) which is derived from (12) must hold for all values of α.

After realization of α , (12) becomes (45).

$$0 \leq E_{DRACurt,d}^{Act,t} \leq E_{DRAMaxCurt,d}^{t} \quad \forall\, d \in [1, D] \tag{45}$$

Inserting (38) into (45), (46) is obtained

$$0 \leq E_{DRACurt,d}^{sch,t} - \gamma_d \alpha \leq E_{DRAMaxCurt,d}^{t} \quad \forall\, d \in [1, D] \quad \forall\, \alpha \in [\alpha^{min}, \alpha^{max}] \tag{46}$$

Since uncertainties in wind, solar and demand for the microgrid are to be handled in the robust model, up and down reserves now cater for only uncertainties in prosumer generation and demand, hence equations (26) and (28) become (47) and (48) respectively.

$$E_{RUR}^{t} = \sum_{p}^{P} \Delta E_{PRGen,p}^{-,t} + \sum_{p}^{P} \Delta E_{PRDem,p}^{+,t} \quad \forall\, t \in [1, T] \tag{47}$$

$$E_{RDR}^{t} = \sum_{p}^{P} \Delta E_{PRGen,p}^{+,t} + \sum_{p}^{P} \Delta E_{PRDem,p}^{-,t} \quad \forall\, t \in [1, T] \tag{48}$$

The resulting robust formulation is therefore made up of expressions (1) through (11), (13) through (25), (27), (29), (44), and (46) through (48).

(46) makes the robust formulation quite challenging to solve, as it should be satisfied for any realization of α within the specified limits. The model is simplified in what follows.

Splitting (46) into two inequality constraints yields:

$$\begin{cases} \gamma_d \alpha \leq E_{DRACurt,d}^{sch,t} \\ \gamma_d \alpha \geq E_{DRACurt,d}^{sch,t} - E_{DRAMaxCurt,d}^{t} \end{cases} \quad \forall\, d \in [1, D] \tag{78}$$

(46) would be satisfied for any realization of α if (50) holds.

$$\begin{cases} \max\limits_{\alpha^{min} \leq \alpha \leq \alpha^{max}} \gamma_d \alpha \leq E_{DRACurt,d}^{sch,t} \\ \min\limits_{\alpha^{min} \leq \alpha \leq \alpha^{max}} \gamma_d \alpha \geq E_{DRACurt,d}^{sch,t} - E_{DRAMaxCurt,d}^{t} \end{cases} \quad \forall\, d \in [1, D] \tag{50}$$

According to Ref. 34, the system in (51) can be decomposed into (52); (52) can also be transformed into (53).[27]

$$\max_{\alpha^{min} \leq \alpha \leq \alpha^{max}} f(\gamma)\alpha \leq a\,; \quad \min_{\alpha^{min} \leq \alpha \leq \alpha^{max}} f(\gamma)\alpha \geq b \tag{51}$$

$$\max(f(\gamma), 0)\, \alpha^{max} + \min(f(\gamma), 0)\, \alpha^{min} \leq a;\ \max(f(\gamma), 0)\, \alpha^{min} + \min(f(\gamma), 0)\, \alpha^{max} \geq b \tag{52}$$

$$\begin{cases} x_1 \alpha^{max} + x_2 \alpha^{min} \leq a;\ x_1 \alpha^{min} + x_2 \alpha^{max} \geq b \\ x_1 \geq 0;\ x_1 \geq f(\gamma);\ x_2 \leq 0;\ x_2 \leq f(\gamma) \end{cases} \tag{53}$$

Hence, (50) is transformed into (54)

$$\begin{cases} x_1^{d,t}\alpha_t^{\min} + x_2^{d,t}\alpha_t^{\max} \geq E_{DRACurt,d}^{sch,t} - E_{DRAMaxCurt,d}^{t} \\ x_1^{d,t}\alpha_t^{\max} + x_2^{d,t}\alpha_t^{\min} \leq E_{DRACurt,d}^{sch,t} \\ x_1^{d,t} \geq 0; x_1^{d,t} \geq \gamma_{d,t};\ x_2^{d,t} \leq 0; x_2^{d,t} \leq \gamma_{d,t} \end{cases} \quad \forall\ t \in [1, T]\ \forall\ d \in [1, D] \tag{54}$$

In the robust formulation, therefore, (46) can be replaced with (54).

3.3 Assumptions

It is assumed that DRA's can implement load curtailment requests within short notice. To keep the model keep the model linear and easy to solve, a linear fuel cost function is assumed for DGs.[1] Also, the microgrid is assumed to span relatively small geographical area, hence, power loss and other power flow equations are not considered.[19]

3.4 Methodology

The developed optimization problem formulation is specified and solved in Advanced Interactive Multidimensional Modelling Systems (AIMMS),[38,39] using its CPLEX 12.6.3 solver.

4. Simulation Setup

In this study, a hypothetical prosumer microgrid similar to that used in Ref. 22 is investigated. The MG demand is met by a combination of diesel generators, wind turbine generators, solar power generators and power from the main grid. Precisely, the MG consists of two DGs (with parameters given in Table I), ten 40 x 250 W solar panels, each with parameters η = 18.6% and S^{PV} = 40 m^2 (similar to that used in Ref. 1), four wind turbines each having a rating of 30 kW, a cut-in speed of 3 m/s, a cut-out speed of 25 m/s and a nominal speed of 12 m/s,[1] an industrial and a commercial prosumer. Installed in the industrial prosumer's site are 4 wind turbines with ratings and characteristics similar to those connected to the microgrid. Also installed in the commercial prosumer's site are ten sets of 40 x 250W solar panels all having specifications similar to those of the microgrid. Each prosumer is assumed to have a battery storage unit co-located with his renewable energy generator, and prosumer battery parameters are shown in Table II. Table III gives details of load reduction offers by DRA's and prosumers. The average forecasts for wind speed is taken from Ref. 1, and that of solar irradiance can be found in Ref. 40. The percentage of peak grid demand forecasts (excluding prosumers' demand) and peak prosumer demand forecasts used in this paper are taken from Refs. 41,42. Peak demands for the microgrid, industrial prosumer and commercial prosumer are assumed to be 400 kW, 150kW and 50kW respectively. The forecasted grid energy price for each interval of the next day is taken from Ref. 1. E_{grid}^{max} is set at 200kWh and r is fixed at 0.15. Percentage forecast errors for wind, solar, and demand are assumed to be 20%, 10% and 1.5%.[22] Three cases are investigated in this work. The advantage of having DRA's is demonstrated by comparing results from the first two case studies (deterministic formulations). In the first case (Case 1), there are no DRA's, hence load reduction offers from small and medium scale users are not considered. DRA's are considered in Case 2 and Case 3, but the robust formulation is studied in the latter.

Table I Diesel generator parameters (Similar to DG parameters in Ref. 1)

Generator	$P_{CG,g}^{min}$(KW)	$P_{CG,g}^{max}$(KW)	a_g($)	b_g($/KWh)	$SC_{DG,g}$($)
1	30	150	0.5	0.053	0.15
2	40	200	0.8	0.068	0.21

Table II Prosumer Battery parameters (Similar to that used in Ref. 22)

	Industrial	Commercial
Battery capacity (kWh)	60 kWh	30 kWh
Minimum energy (kWh)	5 kWh	2.5 kWh
Maximum (dis)charge per interval (kWh)	40 kWh	20 kWh
(Dis)charging efficiency	0.95	0.95
Initial energy content (KWh)	40	30

Table III: Price and quantity offers for load curtailment

Time interval	**DRA 1 quantity offer (KW)**	**DRA 2 quantity offer (KW)**	**Industrial Pro quantity offer (KW)**	**Commercial Pro quantity offer (KW)**
1	15	40	15	0
2	20	45	13	0
3	23	43	15	0
4	25	50	13	0
5	20	50	16	0
6	35	65	11	0
7	45	75	17	0
8	85	125	50	15
9	79	109	40	9
10	88	128	40	5
11	70	100	40	0
12	69	99	40	0
13	72	102	40	7
14	80	110	40	7
15	69	99	40	21
16	78	108	40	7
17	88	118	40	10
18	70	100	11	4
19	69	99	8	15
20	72	102	12	28
21	80	110	14	10
22	20	50	15	3
23	15	45	15	6
24	5	35	12	0
Price offer (Cent/KW)	**5**	**6**	**6**	**7**

5. Results

The results displayed below were generated using a PC with processor characteristics: Intel(R) Pentium (R) Dual CPU T2390 @ 1.86GHz 1.87 GHz. Table IV gives a summary of metrics that show the benefits of having DRA's. The highest power output of DGs, together with the total DG output in each of the three cases investigated is recorded. The Table also shows the resulting MGO cost for each of the cases. Figs. 3 & 4 show the optimal schedules of energy to be bought from the main grid, DG power output and load curtailment for Cases 1 & 2 respectively. Optimal up and down reserve schedules are shown in Figs. 5 & 6 respectively. Figure 7 shows the optimal load curtailment schedules for DRA's and prosumers. To show a balanced grid operation, total power supply and demand

are plotted in Fig. 8. Figs. 9 & 10 show how the MGO's cost changes with respect to the maximum and minimum energy content of prosumers' batteries respectively. Figs 11 & 12 are replicas of Figs. 3 & 7 respectively, but for the robust formulation.

Table IV: Summary of DG output and MGO's cost with and without DRA's

	Case 1 (Without DRA's)	Case 2 (With DRA's)	Case 3 (Robust model)
Max. output of DG1 (KW)	150.00	121.80	137.3592
Max. output of DG2 (KW)	140.64	62.74	0.00
Total output of DGs (KWh)	4623.94	3032.50	2453.72
MGO's cost ($)	486.41	461.76	400.779

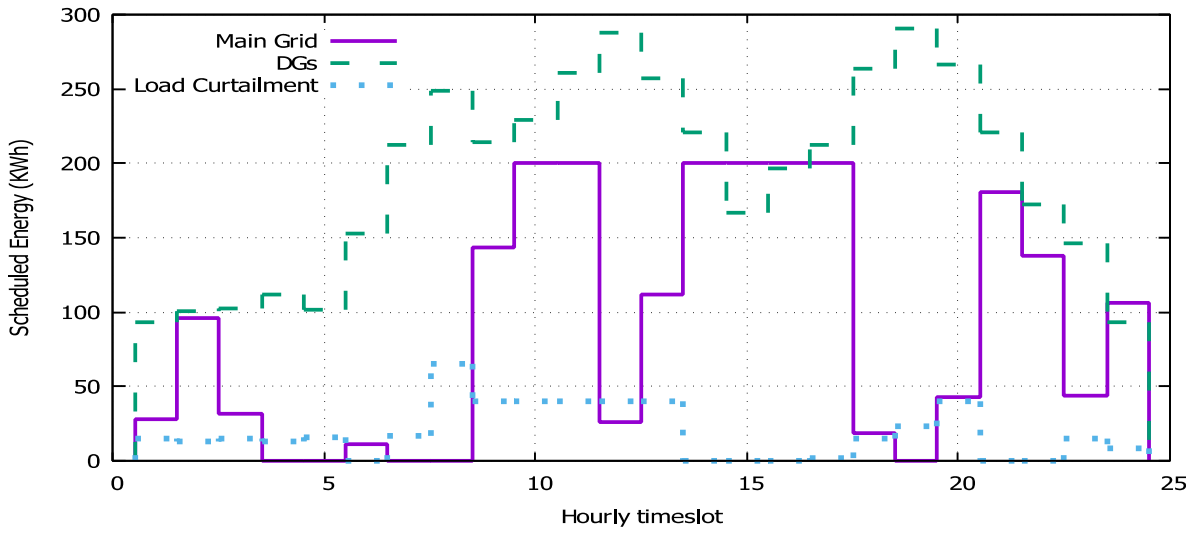

Fig. 3 Optimal energy schedule in Case 1 (No DRA)

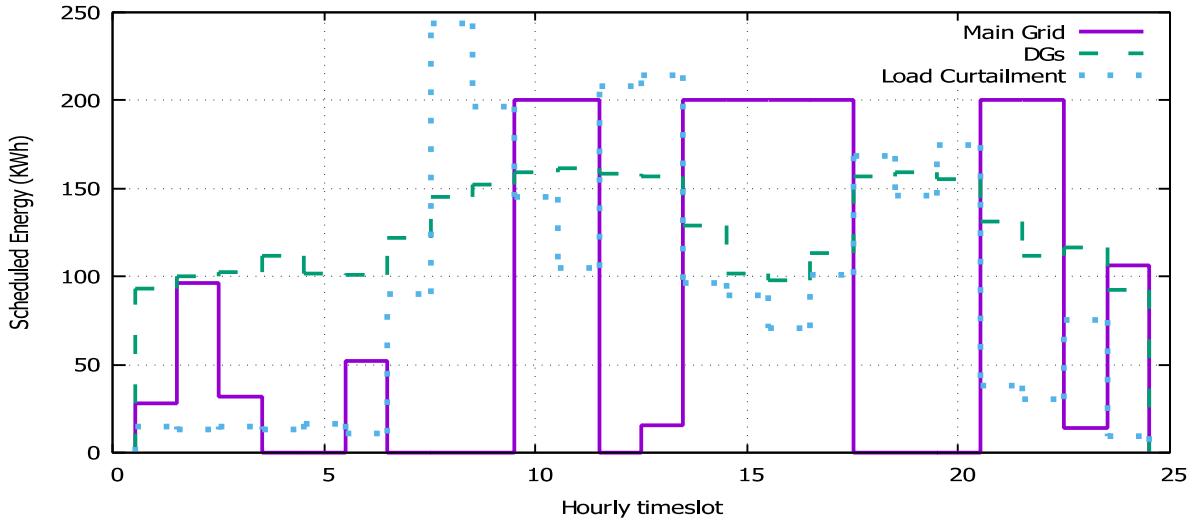

Fig. 4 Optimal energy schedule in Case 2 (DRA's present)

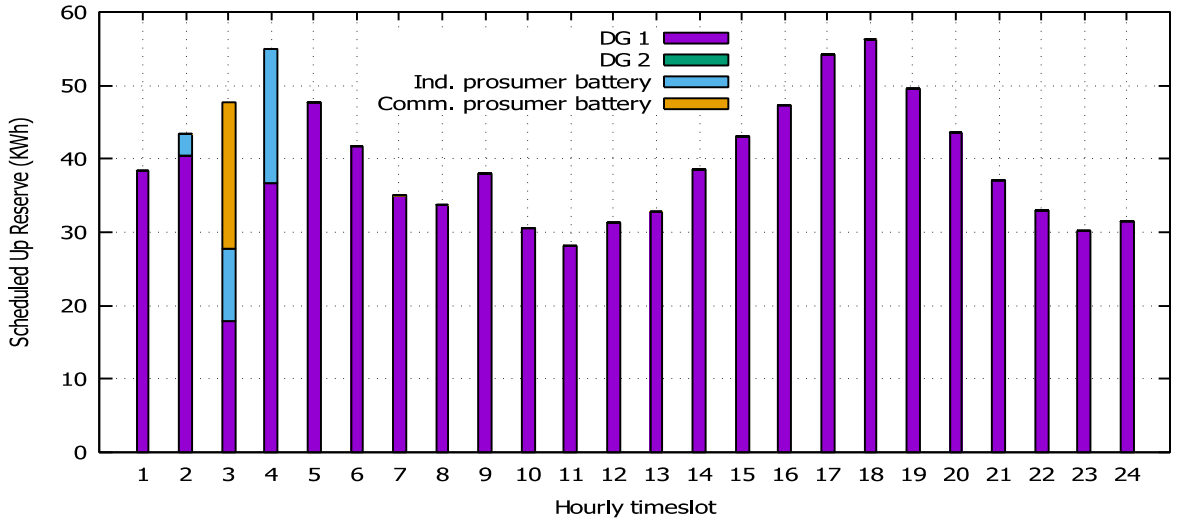

Fig. 5 Optimal up-reserve schedule in Case 2

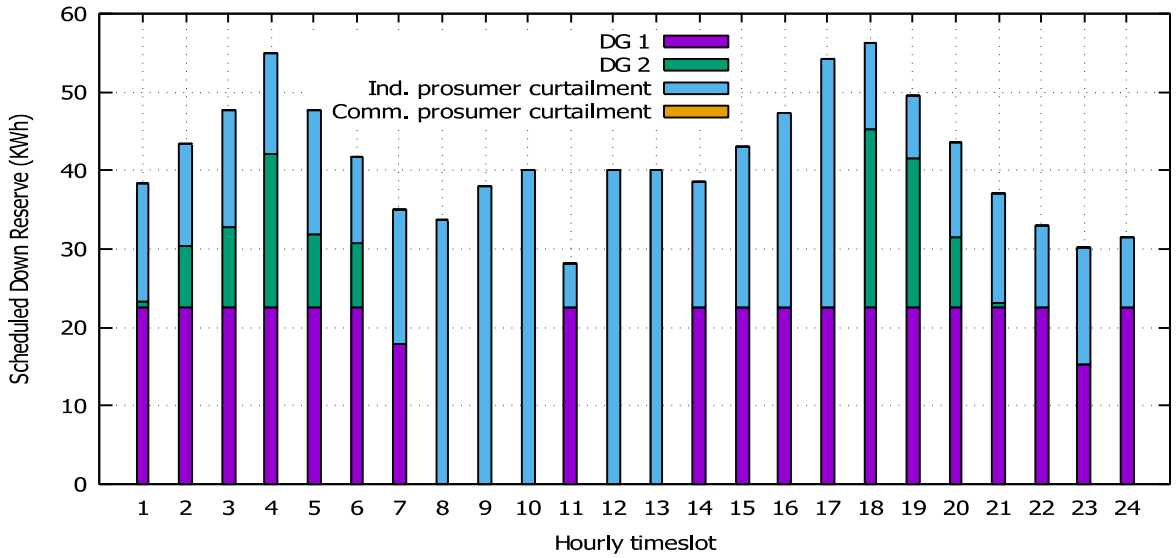

Fig. 6 Optimal down-reserve schedule in Case 2

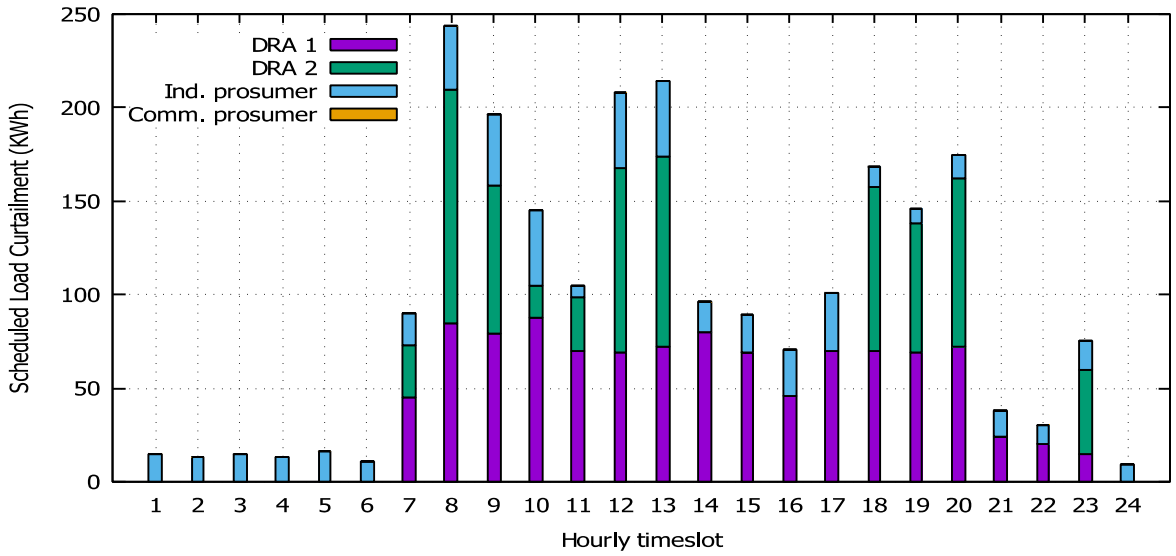

Fig. 7 Optimal load curtailment schedule in Case 2

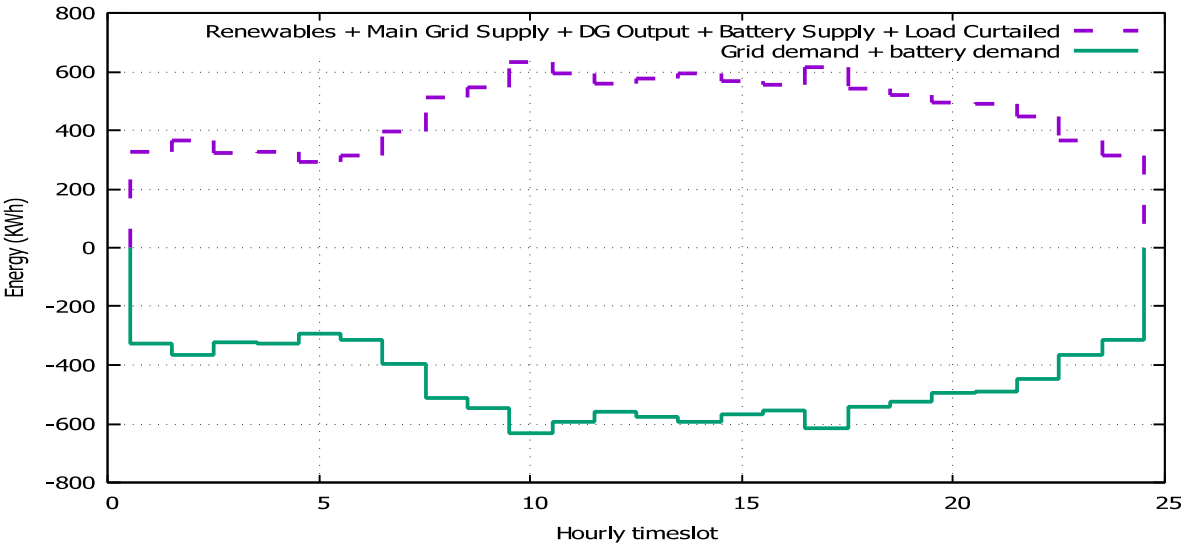

Fig. 8 Aggregate supply and demand schedules showing balanced system operation in Case 2

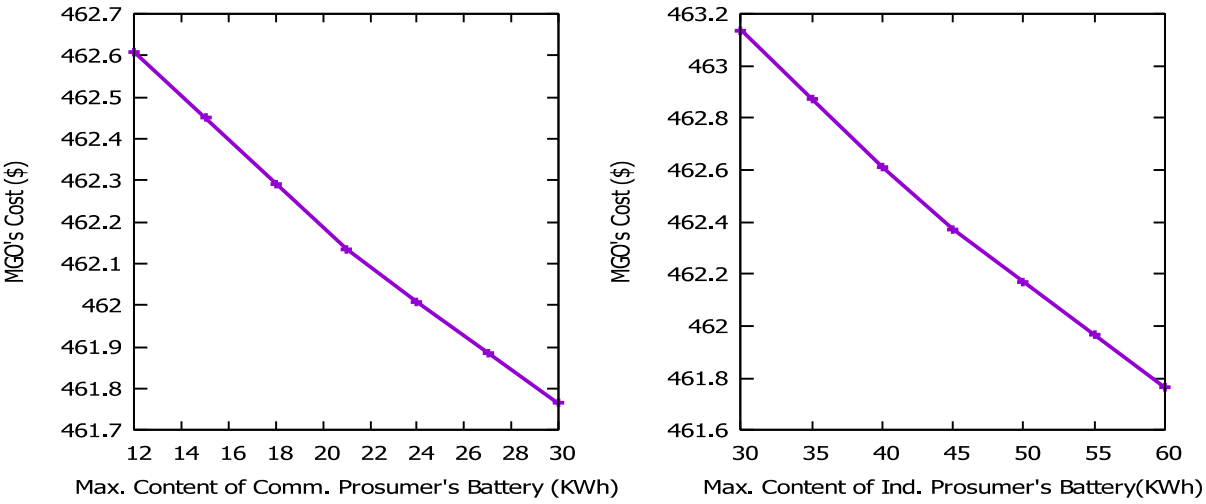

Fig. 9 Change in MGO's cost with respect to maximum energy content of prosumers' batteries (Case 2)

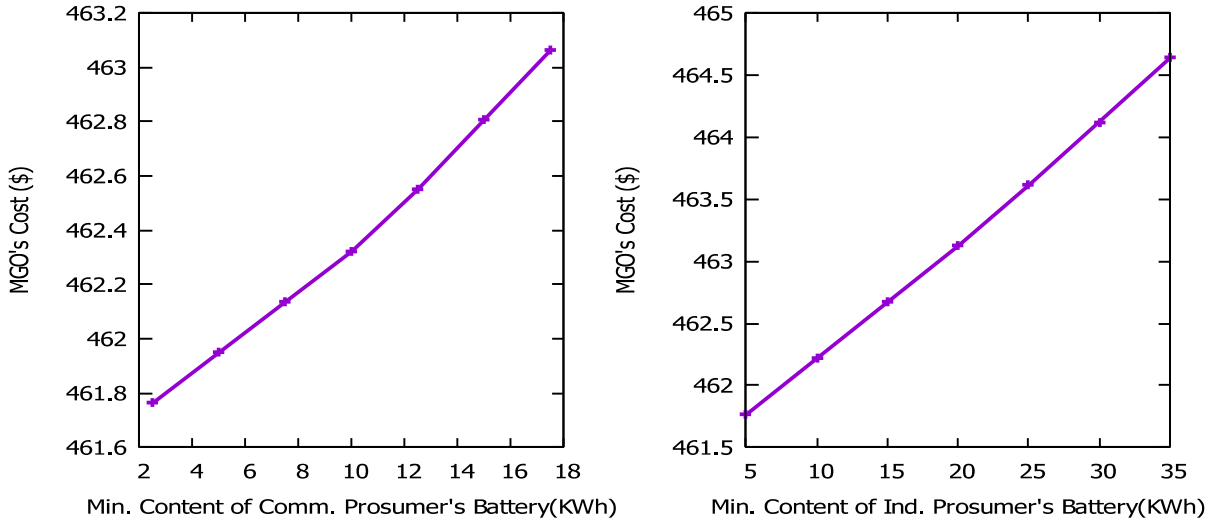

Fig. 10 Change in MGO's cost with respect to minimum energy content of prosumers' batteries (Case 2)

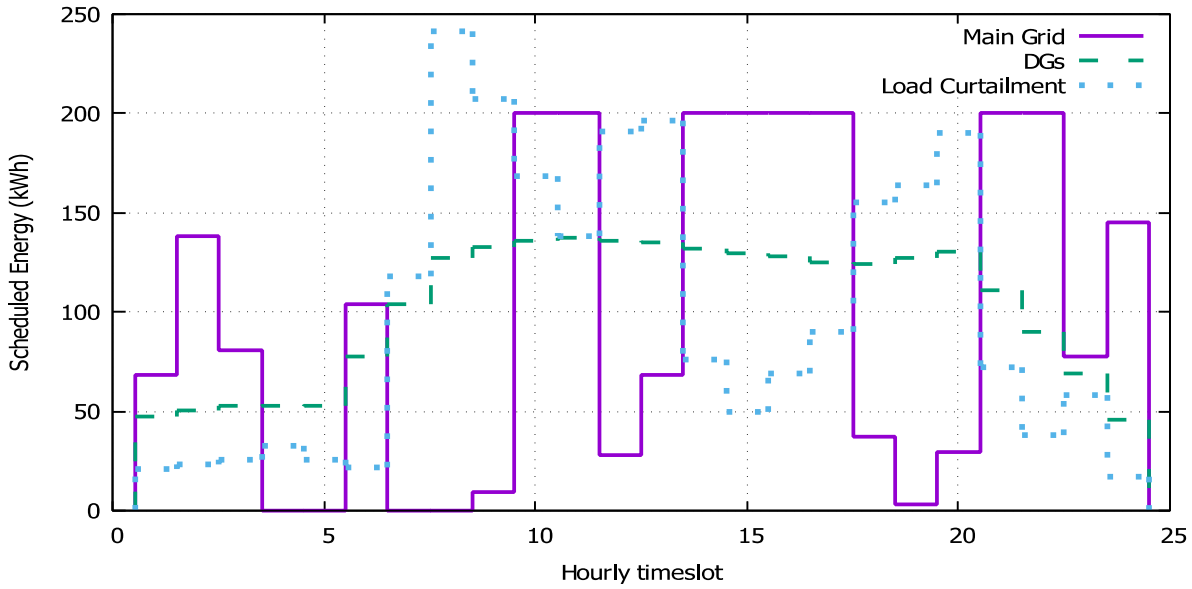

Fig. 11 Optimal energy schedule in Case 3 (Robust formulation)

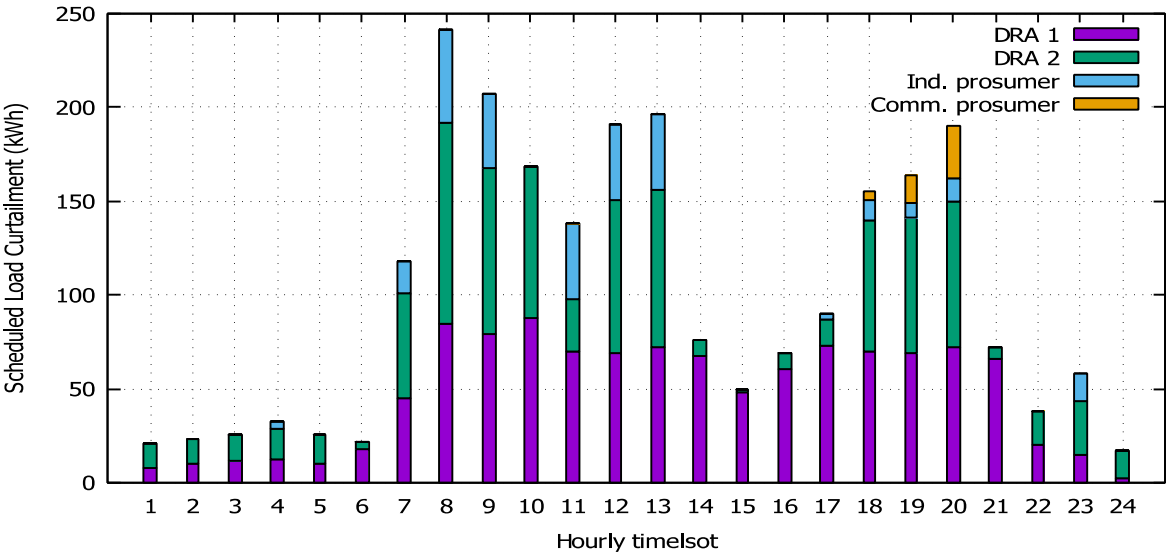

Fig. 12 Optimal load curtailment schedule in Case 3 ((Robust formulation)

6. Discussion of results

Table IV brings to light some benefits of DRA's. Due to the absence of DRA's, the diesel generators are utilized more in Case 1 than in Case 2, resulting in a higher operating cost for the first case. The presence of DRA's in Case 2 gives the MGO more flexible demand resources, resulting in greater scheduling flexibility. In Case 3, the robust formulation is seen to yield the lowest operating cost partly because the reserves set aside for the microgrid's wind, solar and load uncertainties under the deterministic approach are not explicitly provided for in the robust formulation; the total cost of reserves in the deterministic model far outweighs that in the robust model. Notice that total DG output in the robust model is also significantly less than those obtained in the other two cases considered. Comparing Figs. 2 & 11, the aggregate load curtailment, as well as energy purchase from main grid, scheduled over the 24-hour horizon is higher in the robust formulation than in the deterministic counterpart, as a result, DGs have less work to do in the robust formulation. As a matter of fact, DG 2 is not turned on throughout the 24-hour period, in the robust solution.

Comparing the schedules for grid energy purchase shown in Figs. 3 (Case 1) and 4 (Case 2), particularly at intervals with relatively high grid electricity price, reveals another benefit of DRA's. Note that in both figures, load curtailment is represented. While in Fig. 3, load curtailment is performed by large electricity customers alone, load curtailment in Fig. 4 is carried out by large, small and medium scale customers. In timeslots 7, 8 and 19, the price of electricity from the grid is very high; consequently, there is no scheduled grid energy purchase. In Case 1, although electricity price in timeslots 12, 18 and 20 are also relatively high, the MGO is constrained to buy energy from the grid, thereby incurring a relatively high operating cost. However, with the presence of DRA's in Case 2, grid energy purchase is totally avoided during these timeslots. This is made possible by the additional grid balancing resources made available to the MGO by the DRA's.

In the proposed operational dispatch scheme, DGs and prosumer batteries provide the required system up-reserve capacity. By inspecting Fig. 5, it can be seen that most of this capacity, to be provided by DGs, is scheduled to be delivered by DG 1. This is due to its relatively low cost of providing reserve, as compared to that of DG 2.

Down-reserve capacity is provided by DGs and curtailed prosumer loads, and the optimal schedule is shown in Fig. 6. Since no commercial prosumer load reduction offer was accepted, the schedule in Fig. 6 features no capacity from curtailed commercial load.

In Fig. 7, high load curtailments are scheduled for timeslots 8, 12, 18, 19 and 20 due to high electricity prices. In timeslots 9, 10 and 13, relatively high demand and low renewable energy output are responsible for the high load curtailment scheduled. Timeslots 1 through 6 as well as 24 are periods of low electricity price and demand, hence only a small amount of load curtailment offers were accepted. It is interesting to note that although the industrial prosumer's load reduction price offer is not the lowest, only his offers are accepted during these timeslots. The commercial prosumer, being the one with the highest price offer, was not accepted throughout the 24-hour scheduling horizon.

Fig. 8 shows the aggregate energy supply and demand per interval. It can be seen that total energy supplied per timeslot equals that consumed, which portrays power balance in the microgrid at all times. It should be noted that prosumer batteries are taken as demand when they are being charged and as supply during discharging. Total load curtailed can be viewed as negative demand, which in effect is supply.

In the operational dispatch model developed in this study, prosumer batteries are involved in both energy (charging and discharging) and reserve (Up-reserve) scheduling. Prosumers are required to set upper and lower bounds on the amount of energy permitted in their batteries per timeslot, designated respectively as "Max. Content of Comm/Ind. Prosumer's Battery" in Fig. 9 and "Min. Content of Comm/Ind. Prosumer's Battery" in Fig. 10. The effect of these bounds set by prosumers on the operating cost of the microgrid is depicted in Figs. 9 & 10. It noteworthy to mention that although the bounds set by prosumers do not necessarily have to be the same for all timeslots, the results reported graphically in Figs. 9 & 10 were obtained with bounds being the same across the entire scheduling horizon. As seen in Fig. 9, a near-linear line with negative slope describes the relationship between the MGO's cost and upper bounds, for both the industrial and commercial prosumers. In other words, the MGO's cost reduces with increase in upper bound. This is because an increase in upper bound increases the battery capacity available to the MGO which effectively gives him more scheduling flexibility, and consequently reduces operating cost. In Fig. 10 on the other hand, MGO's cost is seen to increase with increase in lower bound, for both prosumers. This is connected to the fact that an increase in lower bound constricts the battery capacity at the MGO's disposal; thereby increasing the microgrid's operating cost.

The robust formulation is such that only DRA load curtailment caters for wind, solar and demand uncertainties. Consequently, as opposed to optimal schedule from the deterministic model, the robust solution schedules at least some amount of DRA curtailment for every timeslot. This is the robust model's way of immunizing its solution against realizations of uncertainties that result in excess energy supply to the MG. Also, comparing Fig. 12 and Table III, it can be observed that the total amount of scheduled DRA curtailment per timeslot is always lower than the maximum offered by the DRA's. The robust solution reserves a portion or all of this extra load curtailment capacity to ensure grid energy balance even when realizations of uncertainties result in energy deficit in the MG.

7. Conclusion

In this paper, an energy and reserve management approach incorporating prosumer behind-the-meter resources and DRA's was developed. In the model, small and medium scale electricity users are involved in the day-ahead operational planning via DRA's. The model was formulated as a mixed integer optimization problem whose solution gives optimal schedules for DG energy outptut, prosumer load curtailment, DRA load curtailment, battery charging and discharging, DG up & down-reserve and prosumer battery reserve. Results obtained from tests carried out for the first two cases investigated bring to light the benefits of DRA's viz. reduction of both microgrid operating cost and DG utilization. A concept taken from CAISO's proposed tariff revisions was also investigated in this paper. While their proposed revision makes allowance for storage facility owners to (1) participate in multiple energy and reserve markets simultaneously, providing energy and/or up & down reserves (2) trade stored energy with neighbours (in networks where such is permitted), it could reduce the amount of grid-balancing resources at the MGO's disposal, thereby increasing the operating cost of the microgrid. The robust formulation reduces the needed contingency reserve capacity thereby reducing the operating cost of the grid. It ensures energy balance in the microgrid whilst immunizing its solution against all possible realizations of uncertainty.

Future work may involve consideration of uncertainties in prosumer import/export. The formulation can also be extended to include environmental constraints viz. greenhouse gas emissions associated with DG generation and battery production.

8. Acknowledgements

Yanxia Sun, the third author of this paper, acknowledges the support received from the South African National Research Foundation Grants (No. 112108 and 112142), South African National Research Foundation Incentive Grant (No. 95687), Eskom Tertiary Education Support Programme (Y. Sun) and research grant from URC of University of Johannesburg.

References

[1]A. Zakariazadeh, S. Jadid, and P. Siano, International Journal of Electrical Power & Energy Systems 63, 523 (2014)

[2]M. Motalleb, M. Thornton, E. Reihani and R. Ghorbani, Applied Energy 179, 985 (2016)

[3]Ž. B. Rejc, M. Čepin, International Journal of Electrical Power & Energy Systems 62, 654 (2014)

[4]S. Borlase, Smart Grids: Infrastructure, Technology, and Solutions. (CRC press; Apr 19, 2016, Boca Raton, Florida, USA).

[5]Y. Chen, M. Keyser, M. H. Tackett and X. Ma, IEEE Transactions on Power Systems 26(2), 829 (2011)

[6]M. Kazemi, H. Zareipour, N. Amjady, W. D Rosehart and M. Ehsan, IEEE Transactions on Sustainable Energy 8(4), 1726 (2017)

[7]E. Sortomme, M. A. El-Sharkawi. IEEE Transactions on Smart Grid 3(1), 351 (2012)

[8]M. Alipour, B. Mohammadi-Ivatloo, M. Moradi-Dalvand and K. Zare, Energy 118, 1168 (2017)

[9]I. Pavić, T. Capuder and I. Kuzle. Applied Energy 157, 60 (2015)

[10]F. Juul, M. Negrete-Pincetic, J. MacDonald and D. Callaway, In Power & Energy Society General Meeting, (2015), Denver, Colorado, pp. 1-5

[11]A. Clausen and G. Ghatikar, In Green Computing Conference (IGCC), (2014), Dallas, Texas USA, pp. 1-10

[12]D. Arnone, A. Barberi, D. La Cascia, E. R. Sanseverino, and G. Zizzo, In Clean Electrical Power (ICCEP), (2015),

Taormina, pp. 170-177.

[13]D. Kottick, M. Blau and D. Edelstein. IEEE Transactions on Energy Conversion 8(3), 455 (1993)

[14]J. Fleer and P. Stenzel. Journal of Energy Storage 8, 320 (2016)

[15]T. Thien, D. Schweer, D. vom Stein, A. Moser, and D. U. Sauer, Journal of Energy Storage 13, 143 (2017)

[16]R. Hollinger, L. M. Diazgranados, F. Braam, T. Erge, G. Bopp and B. Engel, IET Renewable Power Generation 10(1), 63 (2016)

[17]D. Nikolic, M. Negnevitsky and M. De Groot, In Power Generation, Transmission, Distribution and Energy Conversion (MedPower 2016), Mediterranean Conference, (2016), Belgrade, pp. 1-5.

[18]J. Wang, N. E. Redondo and F. D. Galiana, IEEE Transactions on Power Systems 18(4), 1300 (2003)

[19]A. Zakariazadeh and S. Jadid. Journal of Renewable and Sustainable Energy 6(1), 013134 (2014)

[20]A. Zakariazadeh, S. Jadid and P. Siano, Energy Conversion and Management 78, 151 (2014)

[21]V. Mohan, J. G. Singh and W. Ongsakul, Applied energy 160, 28 (2015)

[22]U. Damisa, N. Nwulu and Y. Sun, IET Renewable Power Generation. 12(8), 910 (2018)

[23]S. Golshannavaz, S. Afsharnia, P. Siano. Int J Energy Res 40(11), 1518 (2016)

[24]V.S. Tabar, M.A. Jirdehi, R. Hemmati. Energy 118, 827 (2017)

[25]J. Shen, C. Jiang, Y. Liu, X. Wang. IEEE Access 4, 2349 (2016)

[26]M.C. Hu, S.Y. Lu, Y.H. Chen. Energy 113, 662 (2016)

[27]T. Ding, Z. Wu, J. Lv, Z. Bie, X. Zhang. IEEE Transactions on Sustainable Energy. 7(4), 1547 (2016)

[28]J. Liu, H. Chen, W. Zhang, B. Yurkovich, G. Rizzoni. IEEE Trans Smart Grid 8(6), 2585 (2017)

[29]W.V. Ackooij, R. Zorgati, R. Henrion, A. Möller, See https://www.intechopen.com/books/stochastic-optimization-seeing-the-optimal-for-the-uncertain/chance-constrained-programming-and-its-applications-to-energy-management for Chance Constrained Programming and its Applications to Energy Management, Stochastic Optimization, 2011

[30]A. Ben-Tal, L. El Ghaoui, and A. Nemirovski, Robust Optimization. (Princeton Univ. Press, 2009, Princeton, NJ, USA)

[31]Y. Xiang, J. Liu, Y. Liu. IEEE Trans Smart Grid 7(2), 1034 (2016)

[32]W. Hu, P. Wang, H. Gooi. IEEE Trans Smart Grid 9(2), 1161 (2018)

[33]Y. Guo, C. Zhao. IEEE Trans Smart Grid 9(2), 1301 (2016)

[34]R. A. Jabr, IEEE Trans. Power Systems. 28(4) 4742 (2013)

[35]D. Bertsimas, M. Sim. The price of robustness, Operations Research 52(1), 35 (2004)

[36]156 FERC¶ 61,110 FEDERAL ENERGY REGULATORY COMMISSION WASHINGTON, DC 20426, 2016.

[37]M.F. Zia, E. Elbouchikhi, M. Benbouzid. Applied Energy. (2018).

[38]N.I. Nwulu and X. Xia. Energy 91, 404 (2015)

[39]N.I. Nwulu and X. Xia. Energy Conversion and Management 89, 963 (2015)

[40]D. Q. Hung, N. Mithulananthan and K.Y. Lee. IEEE Transactions on Power Systems 29(6), 3048 (2014)

[41]S. Papathanassiou, N. Hatziargyriou and K. Strunz, In Proceedings of the CIGRE symposium: power systems with dispersed generation (2005), Athens, Greece, pp. 1-8.

[42]R. T. Force. IEEE Trans. on PAS 98(6), 2047 (1979)